

Optimization of Mechanical Ventilator Settings for Pulmonary Disease States

Anup Das, Prathyush P. Menon, Jonathan G. Hardman, and Declan G. Bates*

Abstract—The selection of mechanical ventilator settings that ensure adequate oxygenation and carbon dioxide clearance while minimizing the risk of ventilator-associated lung injury (VALI) is a significant challenge for intensive-care clinicians. Current guidelines are largely based on previous experience combined with recommendations from a limited number of *in vivo* studies whose data are typically more applicable to populations than to individuals suffering from particular diseases of the lung. By combining validated computational models of pulmonary pathophysiology with global optimization algorithms, we generate *in silico* experiments to examine current practice and uncover optimal combinations of ventilator settings for individual patient and disease states. Formulating the problem as a multiobjective, multivariable constrained optimization problem, we compute settings of tidal volume, ventilation rate, inspiratory/expiratory ratio, positive end-expiratory pressure and inspired fraction of oxygen that optimally manage the tradeoffs between ensuring adequate oxygenation and carbon dioxide clearance and minimizing the risk of VALI for different pulmonary disease scenarios.

Index Terms—Computer simulation, lung disease, mechanical ventilation, multiobjective optimization, pulmonary physiology, systems engineering.

I. INTRODUCTION

MECHANICAL ventilation (MV) of the lungs is a commonly-used, life-saving procedure. The majority of critically ill patients in intensive-therapy units (ITU) spend some time with their lungs ventilated with a mechanical ventilator. It is estimated that MV is required by nearly 1.5 million patients in the United States alone every year [1], and indications are that this figure is set to increase [2]. The mortality of patients undergoing ventilation during critical illness is 31–37% [3], [4]. Furthermore, 39% of patients undergo MV for prolonged periods [5], a rate which is also predicted to rise further in the

near future. One of the most problematic issues associated with MV is that it exposes patients' lungs to potentially destructive energy applied by the ventilator [5]–[9]. As a result, ventilator-associated lung injury (VALI) can occur, exacerbating existing conditions, prolonging stays in the ITU and potentially resulting in pneumonia, permanent pulmonary fibrosis, and fatality due to multiple organ failure [6], [9].

To date, very limited progress has been made in the assessment of current practice and the development of better guidelines for MV operators, due to a variety of difficulties. MV administration rates vary with geography, hospitals, resources and ITU operator conditions [10]. There remain differences and ambiguities in the definition of several conditions that lead to the administration of MV. Heterogeneity within the patient population used for clinical trials can dilute any significance gained from these studies. Statistical techniques used in data analysis have been shown not to meet satisfactory standards [11] and incomplete analysis of clinical data can introduce levels of bias and unreliability that produce misleading conclusions [12].

The development of a detailed quantitative understanding of the etiology of VALI also poses significant challenges. Direct measurement of several of the key risk factors for VALI is currently unattainable, and many previous modeling investigations have used only very simplified models, and have not considered crucial factors such as the nonlinearity of alveolar compliance and the closure of alveolar airways [13], [14]. Large peak alveolar pressures have been shown to expose alveoli to the risk of barotrauma [6], [7]. Peak alveolar pressures are related to peak airway pressures, but in diseased lungs with a heterogeneous distribution of time constants the distribution of alveolar peak pressures is impossible to measure clinically. Collapse of the small airways and alveoli (atelectasis) and shear stress caused by repetitive opening and closing of alveoli and the feeding bronchioles can also occur, leading to airway and alveolar injury. Such opening and closing is not seen in normal, healthy lungs, but diseased lungs may be swollen or otherwise impaired such that usually clear passages open only during positive pressure inflation and close again as the inflating pressure is withdrawn.

For MV administration in general, physicians in an ITU aim to maintain the patient's ventilation parameters within regions of "respiratory comfort" [15], [16] based on generic guidelines depending on arterial O_2 – CO_2 levels. Decisions on MV parameters are based on patient outputs and protocol-based mechanical ventilator systems [17] that make no attempt to provide settings which optimize the tradeoffs involved in MV. Rule-based methods (e.g., [18]) are effective, but provide little physiological insight into the reasons for their decisions to the user, and rarely allow multiple variables to be adjusted simultaneously.

Manuscript received July 26, 2012; revised October 2, 2012 and November 26, 2012; accepted December 29, 2012. Date of publication January 11, 2013; date of current version May 15, 2013. This work was supported by the U.K. Engineering and Physical Sciences Research Council under Grant EP/F057016/2 (DGB) and Grant EP/F057059/1 (JGH). *Asterisk indicates corresponding author.*

A. Das and P. P. Menon are with the College of Engineering, Mathematics and Physical Sciences, University of Exeter, Exeter, Devon EX4 4QF, U.K. (e-mail: ad373@exeter.ac.uk; pmp204@exeter.ac.uk).

J. G. Hardman is with the Division of Anaesthesia and Intensive Care, Queen's Medical Centre, University of Nottingham, Nottinghamshire NG7 2RD, U.K. (e-mail: J.Hardman@nottingham.ac.uk).

*D. G. Bates is with the College of Engineering, Mathematics and Physical Sciences, University of Exeter, Exeter, Devon EX4 4QF, U.K. (e-mail: d.g.bates@exeter.ac.uk).

Digital Object Identifier 10.1109/TBME.2013.2239645

The combination of high-fidelity, validated, pathophysiological simulation models with global optimization methods offers a potentially powerful framework with which to address many of the aforesaid difficulties, by performing quantitative “virtual” experiments on an infinitely compliant and strictly controlled *in silico* patient. These experiments may be used to enhance understanding of the causes and pathophysiology of VALI, interrogate the effectiveness of “typical” ventilator parameter settings on different pathologies in different patients, and suggest novel, possibly counterintuitive settings for subsequent testing in clinical trials. A particular advantage of this approach is that it can be used to investigate scenarios where conflicting processes occur and the tradeoffs involved in varying multiple parameters are not intuitively obvious. This is clearly the case for the problem considered here, which requires the management of tradeoffs between oxygenation/ CO_2 clearance objectives and VALI risk factors via simultaneous adjustment of five ventilator parameters: Tidal volume, ventilator rate, ratio of inspiratory to expiratory time, positive end-expiratory pressure (PEEP) and the inspired fraction of oxygen. The aim is to optimize these ventilator settings to minimize the risk factors for VALI, while guaranteeing effective control of arterial oxygenation, carbon dioxide clearance, and pH maintenance.

A number of previous studies have investigated the use of model-based optimization techniques for the assessment of optimal ventilator settings [13], [19]–[23]. These studies have, however, mostly employed very simplified lung models with only two or three compartments. Models of this kind are unlikely to be able to accurately represent the heterogeneity of diseased lung dynamics and the corresponding gas exchange process [24]. Previous studies have also relied on surrogate indicators of lung injury such as peak inspiratory pressure (PIP) [13], [22] that are only representative of global lung dynamics and do not fully utilize the potential of model-based methods to account for local pressure/volume variations. This type of information is particularly relevant to lung pathology where large distributions of time constants and airway pressures may alter the efficacy of the MV process significantly.

The problem considered in this paper corresponds to a multi-variable and multiobjective constrained optimization problem. The dynamics of the ventilator-respiratory system are complex, and include significant nonlinear and nonsmooth properties. Since the possible parameter space for ventilator settings is almost certain to be nonconvex, local gradient-based optimization algorithms are very unlikely to compute globally optimal results and thus we instead employ evolutionary optimization methods that have proven to be effective in solving nonconvex problems with nondifferentiable functions, nonlinearities and stochastic properties, [25], [26]. This study is the first to 1) employ a detailed computer simulation model of lung pathophysiology that has been comprehensively validated both from a clinical [27], [28] and engineering point of view [29], 2) investigate the potential of global multiobjective optimization algorithms, and 3) use the pressures in multiple alveolar units in order to provide a more physiologically relevant indicator of VALI risk.

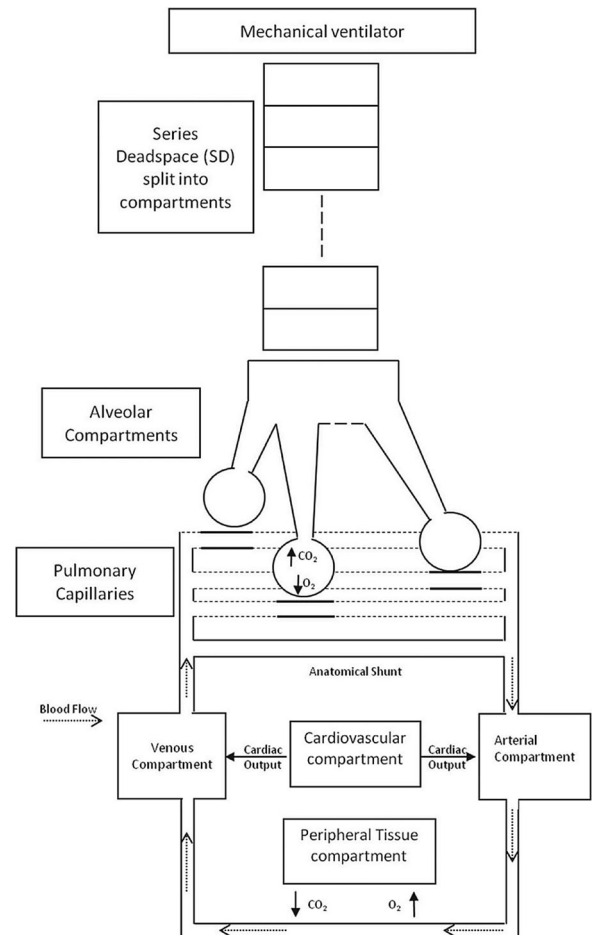


Fig. 1. Diagrammatic representation of the simulation model.

TABLE I
SIGNIFICANT PARAMETERS DESCRIBING MODEL CONFIGURATION

| Configuration | Value |
|---|---------------------------|
| Weight [kg] | 70 |
| Inspired gas | Warmed and humidified air |
| Inspired flow pattern | Constant flow |
| Number of alveolar compartments | 100 |
| Respiratory quotient | 0.8 |
| Oxygen consumption [ml min^{-1}] | 250 |
| Cardiac output [liters min^{-1}] | 5 |

II. SIMULATION MODEL

The simulation model considered in this study is an extended MATLAB implementation of several physiological models originally developed within the Nottingham physiology simulator (NPS) [27], [30]–[32]. The core models in the simulator are designed to represent a dynamic *in vivo* cardio-pulmonary state using a mass-conserving set of equations based on well-established physiological principles. Fig. 1 gives a diagrammatic representation of the model, and some significant parameters indicating the configuration of the model are given in Table I. The simulator has been designed to allow for the observation of gradual

changes in several parameters that are otherwise difficult to estimate *in vivo*.

The lungs are modeled as a dynamical system comprising external equipment (i.e., a mechanical ventilator), anatomical and alveolar deadspaces, and ventilated, perfused alveoli. In this study, 100 heterogeneous alveolar compartments have been incorporated into the model. The inspired air consists of oxygen (19.6%), nitrogen (74%), and carbon dioxide (0.1%). The balance is made up of water vapor (6.3%) present due to the humidification of air, which is assumed to be at a temperature of 37 °C. The model obeys ideal gas laws and incorporates the effect on gas flow of the temperature difference between inspired gas and core body temperature. In the model, complete mixing of gases in the alveoli is assumed. Simulating the movement of oxygen, carbon dioxide, and nitrogen causes changes in lung volume and resulting gas concentrations. Blood flow through the lung is divided into shunted or nonshunted blood. Blood flow across the alveoli is time-sliced, such that each individual packet of blood comes to equilibrium with alveolar gases through an iterative movement of gas between alveolar and capillary compartments. Previous validation studies using clinical data have shown that the equilibration process as simulated in our model provides a mean prediction error of 0.05 kPa for partial pressure of oxygen P_{aO_2} and 0.09 kPa for partial pressure of carbon dioxide P_{aCO_2} [28], for patients suffering from severe respiratory distress.

Calculation of blood oxygen and carbon dioxide content after equilibration uses standard formulas and includes the effects of base excess, temperature, and plasma pH in the internal blood–gas calculations. The plasma pH depends on the base excess, temperature, and plasma carbon dioxide content. Humidification and temperature effects on the inspired dry air concentrations are also incorporated. Barometric pressure, or the atmospheric pressure, is taken to be at 101.3 kPa. Peripheral metabolism involves simple production of carbon dioxide and extraction of oxygen, using oxygen consumption, respiratory quotient, and cardiac output. The bronchiolar flow can be laminar or turbulent, a common resistance to flow is included, and bronchiolar resistance variations as a result of expansion of the lungs are also included. The type of inspiratory flow during MV of the lungs can be preset to constant-flow or constant-pressure; constant-flow is considered in this study.

III. SIMULATING DISEASE STATES

The simulated lung in the model consists of 100 parallel alveolar compartments, each of which is assigned an individual bronchiolar inlet resistance (BIR). Each alveolar compartment has a corresponding pulmonary capillary compartment with a pulmonary vascular resistance (PVR). The primary goal of the respiratory system is the transfer of gases into and from the blood across the alveolar membrane. To satisfy this requirement optimally, the amount of gas (ventilation, V) and blood (perfusion, Q) taking part in the gas exchange needs to be matched. In many pulmonary diseases, alveolar mismatching can be the most influential mechanism in causing abnormal arterial blood gases.

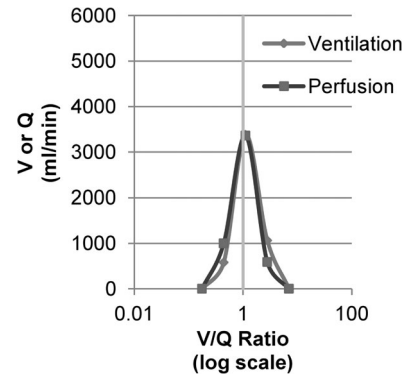


Fig. 2. Ventilation perfusion distribution (VQ) of the simulated healthy lung. Lines are drawn as a visual aide only.

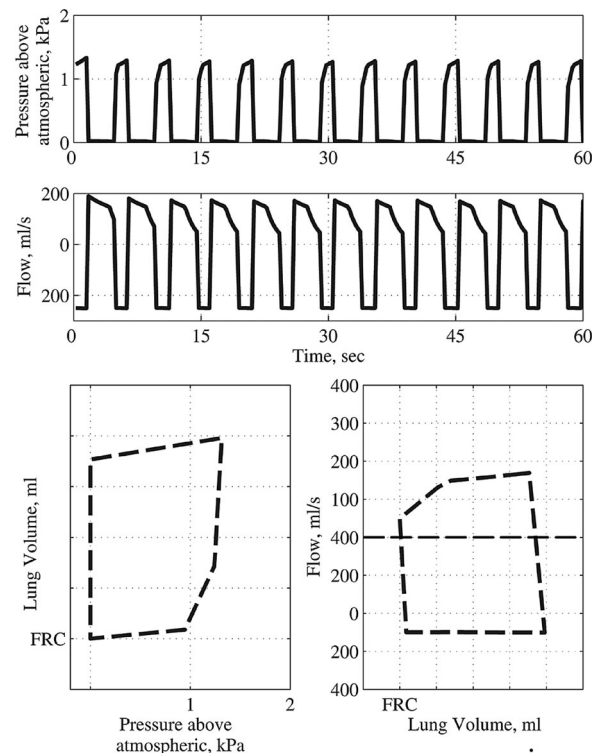


Fig. 3. Lung pressure, flow and volume characteristics of a simulated healthy lung. Figure plotted using tidal volume = 400 ml, ventilator rate = 12.5 bpm and inspiratory to expiratory ratio = 1/3 and the mechanical ventilator set to “constant flow”.

For a healthy lung, the parameters BIR and PVR are randomly distributed in the model with a uniform distribution of $U(0.75x, 2x)$ where x is $BIR_{nominal}$ (0.001 kPa/ml/min) and $PVR_{nominal}$ (16 ml/min), respectively, to allow the simulation of a heterogeneous ventilation perfusion (V/Q) distribution, as proposed in [33]. Fig. 2 shows the VQ plot for a healthy lung produced by the model. Each point shows a specific amount of ventilation or perfusion at its respective VQ ratio. Total flows can be calculated by adding the individual data points. As shown, the healthy lung VQ distribution is unimodal, approximately symmetric, and clustered fairly tightly around a VQ ratio of 1. Fig. 3 presents the pressure, flow, and volume features of the simulated healthy lung. Figs. 2 and 3 are produced using standard

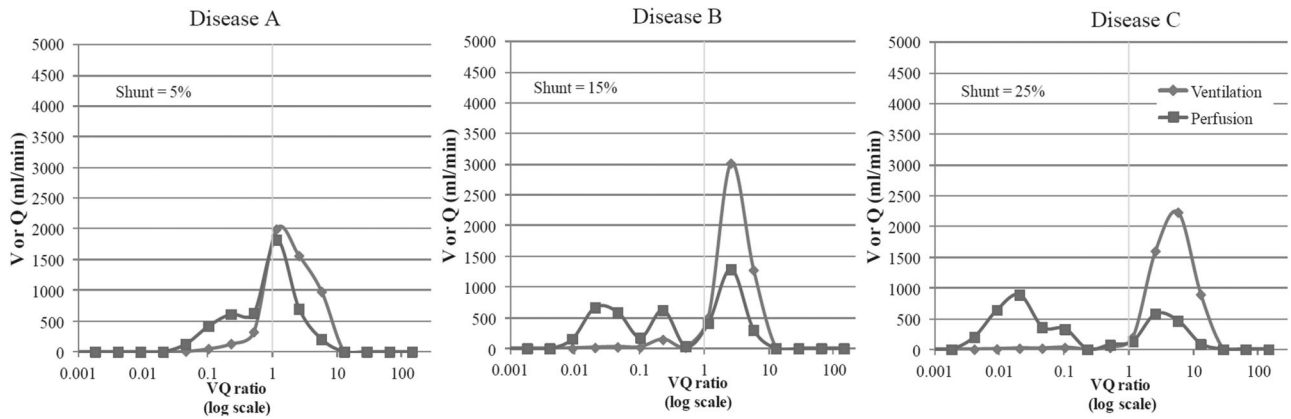


Fig. 4. Ventilation perfusion curves of different simulated pulmonary diseases. The plots describe variation in distribution of gas exchange across the lung. Values for shunt refer to total calculated shunt fraction.

TABLE II
CONFIGURATION OF “VIRTUAL” PATIENTS

| | BIR | PVR | SHUNT |
|-----------|------------------------|---------------------|-------|
| Disease A | 100-1 50-20 1-50 1-100 | 1-1 1-60 2-80 4-100 | 5% |
| Disease B | 500-1 1-50 1-100 | 1-1 1-80 4-100 | 15% |
| Disease C | 800-1 1-50 1-100 | 1-1 1-50 12-100 | 25% |

The VQ defects were configured by adjusting the bronchial (BIR) and vascular (PVR) resistances in the model and shunt. The values are given as X-Y, where X is the factor by which the resistance was multiplied and Y is the alveolar compartment number. So “100-1 10-50” denotes that between compartment number 1 and 50, the distribution of resistance multipliers were between 100 and 10. The ranges of BIR and PVR conformed to the ranges considered in a previous study [38], with the only limitation that the total airway resistance R_{aw} of the diseased lung is less than five times the R_{aw} of normal lung (within the bounds given in [39]) and the total pulmonary vascular resistance (TPVR) is less than five times the TPVR of a normal lung (within the bounds given in [40]).

mechanical ventilator settings of tidal volume = 400 ml, ventilator rate = 12.5 bpm, and inspiratory to expiratory ratio = 1/3.

Virtual representations of diseased lungs can be simulated in the model by creating abnormal V/Q distributions. Abnormal V/Q distribution in the lung results from the obstruction of air flow and blood flow since in diseased lungs alveolar compartments will have reduced ventilation because of extreme narrowing of the inlet (bronchial) airways. These correspond to alveolar compartments with high BIR, reduced ventilation and low alveolar volumes. Abnormal V/Q distribution has been shown to exist in pulmonary diseases such as chronic obstructive pulmonary disease (COPD) [34], asthma [35], pulmonary embolism [36], and acute respiratory distress syndrome (ARDS) [37]. These distributions are configured in the model by increasing the magnitudes of the BIR and PVR of the alveolar and capillary compartments, using the same method described in [38], with values given in Table II. To capture the heterogeneity of alveolar compartments we again scatter these values using a uniform distribution over the 100 compartments. The resulting VQ mismatch for three different disease states, of progressively increasing severity, is shown in Fig. 4. Fig. 5 shows the pressure-volume and flow-volume relationship of a diseased lung (disease B from Fig. 4), which should be compared to the relationships for a healthy lung shown in Fig. 2.

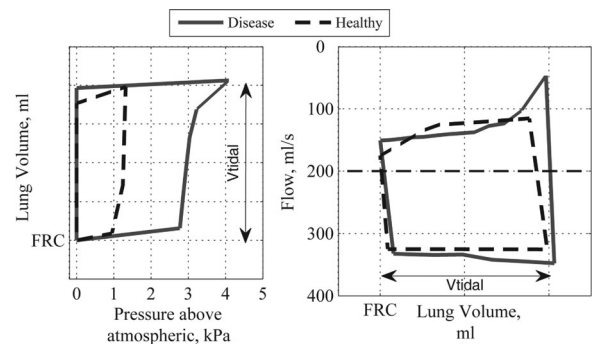


Fig. 5. Pressure-volume and flow-volume loops of a simulated disease lung. Disease B from Fig. 6 compared to that of a healthy lung.

TABLE III
PHYSIOLOGICAL PARAMETERS FOR THE DISEASE CASES IN FIG. 6 UNDER NOMINAL VENTILATOR SETTINGS OF TIDAL VOLUME = 400 ML, VENTILATOR RATE = 12.5 BPM, INSPIRATORY TO EXPIRATORY RATIO = 1/3, PEEP = 0 CMH₂O AND FIO₂ = 0.21

| | P_{av} [kpa] | P_{aCO_2} [kpa] | P_{aO_2} [kpa] | pH |
|-----------|----------------|-------------------|------------------|-------|
| Disease A | 1.15 | 5.81 | 7.71 | 7.387 |
| Disease B | 1.56 | 6.02 | 5.17 | 7.354 |
| Disease C | 1.03 | 6.49 | 3.72 | 7.324 |

Table III provides the values of the physiological parameters produced under these disease cases when the MV parameters remain at their nominal values. It is clearly evident that as the severity of the disease increases, the arterial oxygen partial pressure falls and arterial carbon dioxide rises. Indeed, the value of P_{aO_2} in all three cases is lower than its minimum allowable value.

IV. FORMULATING THE CHOICE OF VENTILATOR PARAMETER SETTINGS AS AN OPTIMIZATION PROBLEM

In this study, the following five key ventilator settings are considered as variable parameters that may be adjusted to optimize the tradeoff between effective gas exchange and minimizing the risk of VALI.

- 1) Tidal volume (V_{tidal} , [ml]): The volume of air traveling in or out of the patient’s lungs during every breath.

TABLE IV
MECHANICAL VENTILATOR PARAMETERS,
THEIR BOUNDS AND NOMINAL VALUES

| Parameter X | Lower Bound lb | Upper Bound ub | Nominal |
|---------------------------|---------------------|---------------------|---------|
| Vtidal [ml] | 280 | 840 | 400 |
| VentRate [bpm] | 6 | 35 | 12.5 |
| I:E | 0.25 | 0.8 | 0.33 |
| PEEP [cmH ₂ O] | 0 | 24 | 0 |
| FIO ₂ | 0.21 | 1 | 0.21 |

- 2) Ventilation rate (VentRate, [breaths/min]): The number of breaths per minute.
- 3) Duty cycle (I:E): The ratio of inspiratory time to total ventilatory cycle duration.
- 4) Positive end-expiratory pressure (PEEP, [cmH₂O]): The positive pressure in the lungs at the end of exhalation.
- 5) Fraction of inspired oxygen (FIO₂): The fraction of oxygen constituting the inhaled volume of gas as provided by the mechanical ventilator. High values of FIO₂ can straightforwardly improve oxygen levels but they can also cause collapse in the alveolar regions as oxygen is rapidly absorbed into the blood, reducing alveolar volume below critical collapsing volume. Studies [41], [42] have shown that increased FIO₂ should be accompanied by an increase in PEEP to prevent collapse. In this paper, the optimization algorithm attempts to minimize FIO₂, effectively requiring the least amount of supplemental oxygen needed to satisfy gas exchange requirements.

Data available from clinical trials [3], [41], [43], show considerable variations in the allowable ranges for MV settings in the ICU. For the purpose of this study, maximum allowable ranges of variation for the values of these parameters have been defined based on current clinical practice and to be consistent with these studies. Vtidal is allowed to vary within a range from 280 to 840 ml, corresponding to 4–12 ml/kg for a body weight of 70 kg. VentRate is bounded within the range 6–35 breaths/min, I:E is limited to the interval 0.25–0.8 (i.e., a ratio between 1:3 and 4:1), PEEP is constrained within 0–24 cmH₂O and FIO₂ is bounded within 0.21–1. All of these parameters are also assigned “typical” nominal values, which are used to derive their respective VQ distributions (see Figs. 2 and 4). A summary is provided in Table IV.

Maximum and/or minimum allowable values are also defined for several key physiological indicators that are returned as outputs by the model. To monitor effective arterial oxygenation, partial pressure of oxygen, P_{aO_2} , needs to be considered. In order to maintain effective arterial oxygenation, P_{aO_2} is constrained to be higher than 8 kPa. Arterial partial pressure of carbon dioxide, P_{aCO_2} is another key indicator of alveolar ventilation that also indirectly reflects acid-base balance. P_{aCO_2} is constrained to be between 4 and 8 kPa. The risk of barotrauma is proportional to the peak alveolar pressure, (P_{alv} , kPa above atmospheric pressure) in any alveolar unit, and thus P_{alv} is limited to 4 kPa. The values of all these parameters are recorded after a physiological time simulation of 20 min. At the end of the

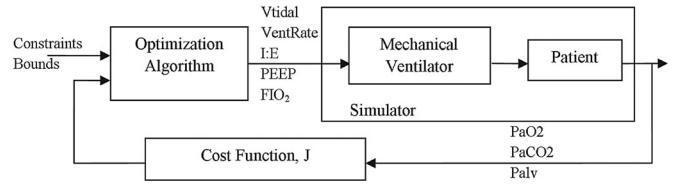


Fig. 6. Schematic diagram of the optimization framework.

TABLE V
SELECTED PHYSIOLOGICAL INDICATORS, THEIR ACCEPTABLE RANGES
AND DESIRED VALUES

| Physiological parameters | Acceptable values | Desired |
|--------------------------|-------------------|---------|
| P_{alv} [kPa] | < 4 | 0 |
| P_{aO_2} [kPa] | > 8 | 10 |
| P_{aCO_2} [kPa] | > 4, < 8 | 5 |

P_{alv} refers to peak pressure in kilopascals (kPa) above atmospheric pressure.

20-min period, mean values of P_{aO_2} and P_{aCO_2} are computed over the last 2 min (representing the final 10% of data). P_{alv} is calculated as the average of the peak pressure in the most highly-pressurized 20% of all alveoli over the final 2 min of the simulation. Ventilation perfusion plots are drawn with total ventilation and perfusion recorded across the 100 alveolar units at the end of a simulation.

A schematic representation of the proposed *in silico* optimization framework is shown in Fig. 6. The optimization problem can be formulated mathematically as follows:

$$\min_x J(f(x))$$

subject to the following constraints:

$$4 \leq P_{aCO_2} \leq 8, P_{aO_2} \geq 8, P_{alv} \leq 4, lb \leq x \leq ub.$$

In this formulation, J represents the objective function for the optimization problem, $f(x)$ represents the simulation model, and x is a vector containing the values of the optimization parameters (i.e., the ventilator settings). The optimization algorithm searches for values of the parameters x , between their lower (lb) and upper (ub) bounds, that minimize J . To capture the tradeoff inherent in the problem, the normalized aggregated objective function J is defined as

$$J = J1 + J2$$

where

$$J1 = w_1 \frac{P_{alv}}{r_1}, J2 = w_2 \left(\frac{|P_{aCO_2} - 5|}{r_2} + \frac{|P_{aO_2} - 10|}{r_3} \right).$$

Thus, large values of $J1$ will be produced by combinations of ventilator settings that cause high peak alveolar pressures (and hence increase the risk of VALI) while large values of $J2$ reflect settings that provide poor gas exchange. The parameters r_1 , r_2 , and r_3 are used to approximately normalize the different output parameters and are determined by the maximum difference between acceptable values and desired values given in Table V. w_1 and w_2 are the weights whose default values are set equal to 1 but whose values can be adjusted to explore the effects of prioritizing different criteria on the computed settings. For

TABLE VI
NOMINAL AND OPTIMAL SETTINGS AND THE RESULTING PHYSIOLOGICAL
PARAMETERS FOR THE HEALTHY LUNG MODEL

| | | Nominal | Optimized |
|--------------------------------|---------------------------|---------|-----------|
| Mechanical Ventilator Settings | Vtidal [ml] | 400 | 304 |
| | VentRate [bpm] | 12.5 | 10.3 |
| | I:E | 0.33 | 0.32 |
| | PEEP [cmH ₂ O] | 0 | 0.4 |
| Outputs | FIO ₂ | 0.21 | 0.22 |
| | P_{alv} [kPa] | 0.80 | 0.67 |
| | P_{aCO_2} [kPa] | 5.44 | 6.45 |
| | P_{aO_2} [kPa] | 13.03 | 9.98 |

example, increasing w_2 relative to w_1 causes the optimization algorithm to search for solutions that minimize J_2 more than J_1 . If the patient is exhibiting lower than required oxygenation, the MV operator thus has the option to tailor the optimization toward improving oxygenation at the cost of generating a higher value of P_{alv} .

Since the values of the optimization parameters vary significantly in magnitude (e.g., Vtidal is several hundred times larger than IE), they must also be normalized to avoid numerical problems with the chosen optimization routines. All five parameters are thus allowed to vary within their bounds (see Table IV), normalized between -1 and 1 . For the normalized aggregated objective function, a hybrid optimization algorithm combining a genetic algorithm (GA) [25] with a pattern search algorithm known as mesh adaptive direct search (MADS) [26] was used to find the globally optimal solution x_{opt} . The GA starts with an initial randomly chosen population of candidate solutions. Based on past experience and some initial exploratory studies, we chose a population size of 30. The algorithm terminates when the total number of generations exceeds 20. The result from the GA is used to initiate the MADS algorithm, which terminates if the magnitude of the objective function value improves by less than a preset tolerance, chosen as 10^{-3} , or if the total number of function evaluations by the algorithm exceeds 600. To validate this solution and further investigate the tradeoffs involved in this problem, a multi-objective global optimization algorithm, NSGA-II [44], was also used to compute an estimate of the Pareto-optimal front corresponding to all possible solutions for different choices of the weighting functions w_1 and w_2 . NSGA-II was initiated with a population size of 30 and allowed to evolve for 60 generations.

V. RESULTS

A comparison of the results obtained with the nominal and optimized ventilator parameters for the healthy lung model is shown in Table VI. Compared with the nominal settings, the optimization algorithm has sought to find a combination of ventilator parameters that pushes down the value of P_{alv} , at the cost of slightly increasing P_{aCO_2} and reducing P_{aO_2} (while still keeping these parameters within their specified bounds). It has achieved this principally by reducing Vtidal, as would be expected from normal clinical practice. “Re-balanced” settings which give a higher priority to gas exchange could easily be

TABLE VII
OPTIMAL SETTINGS AND THE RESULTING PHYSIOLOGICAL PARAMETERS FOR
THREE DISEASE CASES

| | | Disease A | Disease B | Disease C |
|--------------------------------|---------------------------|-----------|-----------|-----------|
| Mechanical Ventilator Settings | Vtidal [ml] | 419 | 412 | 378 |
| | VentRate [bpm] | 14.03 | 20.45 | 31.86 |
| | I:E | 0.28 | 0.54 | 0.33 |
| | PEEP [cmH ₂ O] | 1.8 | 3.9 | 7.5 |
| Outputs | FIO ₂ | 0.30 | 0.29 | 0.81 |
| | P_{alv} [kPa] | 1.95 | 1.96 | 3.82 |
| | P_{aCO_2} [kPa] | 5.43 | 4.52 | 5.06 |
| | P_{aO_2} [kPa] | 10.00 | 10.25 | 9.99 |

TABLE VIII
COMPARISON OF RESULTS FOR DISEASE CASE B WITH DIFFERENT OBJECTIVE
FUNCTION WEIGHTS

| | Weight w_j | $w_j=1$ | $w_j=10$ |
|--------------------------------|---------------------------|---------|----------|
| Mechanical Ventilator Settings | Vtidal [ml] | 412 | 447 |
| | VentRate [bpm] | 20.45 | 7.88 |
| | I:E | 0.55 | 0.3 |
| | PEEP [cmH ₂ O] | 3.9 | 1 |
| Outputs | FIO ₂ | 0.29 | 0.75 |
| | P_{alv} [kPa] | 1.96 | 0.98 |
| | P_{aCO_2} [kPa] | 4.52 | 7.50 |
| | P_{aO_2} [kPa] | 10.25 | 9.90 |

computed by adjusting the weights w_1 and w_2 in the objective function for the optimization algorithm.

Table VII summarizes the values of the optimal settings for each individual disease case with their corresponding physiological parameters. When compared with the results of applying the nominal settings for each disease state (Table II), it is clear that the optimized settings provide a marked improvement in the values of the physiological parameters. In particular, note that the value of P_{aO_2} has now increased to lie within its allowable range for all three cases. This improvement in oxygenation has been achieved at the cost of an increase in the value of P_{alv} , but even for the most severe case P_{alv} still remains lower than its maximum limit.

Further “fine-tuning” of the ventilator settings can be easily achieved by adjusting the weights w_1 and w_2 in the objective function and re-running the optimization algorithm. For example, Table VIII shows the effect on the optimal settings for disease case B of making w_1 equal to 10 while leaving w_2 at its nominal value of 1. This has the effect of making the value of P_{alv} the dominant term in the objective function, so that the optimization algorithm tries to find settings that reduce its value by a larger amount. As shown in Table VII, the effect of this re-balancing is to reduce P_{alv} from 1.96 to 0.98 kPa, at the cost of an increase in P_{aCO_2} and a small decrease in P_{aO_2} (although both these parameters still remain within their allowable ranges). The set of 30 solutions returned by the multiobjective NSGA-II algorithm, together with the optimal solutions given in Table VIII, is shown in Fig. 7. It is evident that the previous

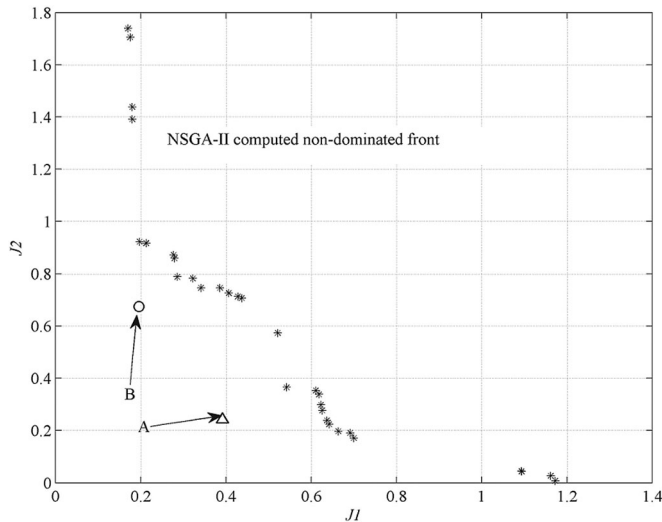


Fig. 7. Set of optimal solutions generated by NSGA-II compared to the results of Table VII. Point “A” is the solution with weights $w_1 = w_2 = 1$ and point “B” is the solution with weights $w_1 = 10$ and $w_2 = 1$.

solutions lie on the appropriate sections of the nondominated front computed by the NSGA-II algorithm.

VI. DISCUSSION

Poor oxygenation of the blood and resultant hypoxia can be fatal to patients in an ITU. Carbon dioxide (CO_2) clearance from the blood is also essential as excessive CO_2 in the blood can lead to acid base imbalance, risking serious damage to the major organ systems. Traditionally, MV operators have focused on ensuring that oxygenation requirements are adequately met and carbon dioxide clearance is maintained. In recent years, however, the increasing incidence of VALI, which has been attributed to the occurrence of high pressures and volumes in the alveoli, has led MV operators to be more cautious and to consider other physiological factors which previously tended to be ignored. The objective of minimizing the risk of VALI can often be in direct conflict with the traditional aim of ensuring good gas exchange, and optimal settings that satisfy both sets of criteria can be difficult to predict.

The optimal settings for the different disease scenarios presented here are shown to satisfy the clinical objectives of 1) maintaining adequate oxygenation, 2) maintaining adequate carbon dioxide clearance, and 3) minimizing the risks of VALI. Interestingly, the optimal settings not only optimize the particular parameters contained in the objective function, but also act to more generally improve the gas exchange within the lung. Fig. 8 plots VQ distributions under the computed optimal settings for the three disease cases. In comparison to VQ distributions under nominal settings of Fig. 4, significant improvement is evident in all cases, where the optimal setting causes the gas exchange to shift toward a VQ ratio of 1. Under nominal settings, there are a large number of perfused alveoli where little gas exchange occurs due to under-ventilated or collapsed airways. From Fig. 8 and Table VII, it is evident that the higher values of ventilator rate, I:E ratio and PEEP act to improve the ventilation to

these areas of the lung where there is poor gas flow, which in turn improves the VQ mismatch and helps achieve better gas exchange.

An important objective to consider when searching for optimal ventilator settings is to reduce the risk of hypercapnia (by lowering PaCO_2 as closely as possible to its desired value of 5 kPa). In the ITU, the physician may sometimes prefer to focus only on the pH value and reduce the risk of lung injury while allowing an increase in PaCO_2 (permissive hypercapnia). This can be a common strategy in patients with severe respiratory distress [45]. In this case, the objective function for our optimization problem can easily be altered to include pH instead of PaCO_2 . However due to the standard pH PCO_2 relationship, achieving a stable PaCO_2 value would normally be expected to effectively satisfy the pH requirements of the patient. For example, disease C has a value of 7.354 for pH (see Table III). Under the optimal settings of Table VII, however, pH was returned to a normal value of 7.41. Thus, there may not be a significant benefit in considering pH above PaCO_2 as a direct optimization target.

The model used in this study is based on several assumptions, e.g., the simulated patient is assumed to be under complete MV with the effects of ventilatory autoregulation not incorporated. The model also does not consider any metabolic, myogenic, or neurogenic autoregulation of the physiological parameters. Clearly, such assumptions would need to be addressed before any direct bedside application could be considered, and further development of the model along these lines is currently underway. On the other hand, with respect to previous studies [13], [20], [22], the present model does incorporate the effect of many key mechanisms, such as the gas exchange process across the alveolar-capillary membrane, the variable heterogeneous distribution of both ventilation and perfusion, the effect of airway and vascular obstruction, hypoxic pulmonary vasoconstriction, and the recruitment and de-recruitment of alveolar units, among others. The model has also been applied previously in representing severe pulmonary pathological scenarios such as ARDS [28], [38] and hypoxemia [46].

In this study, we simulated three different lung conditions representing disease states of increasing severity, which could be realistically found in patients in an ITU. The disease states were obtained by altering the ventilation and perfusion characteristic within the model. Patients suffering from severe respiratory distress requiring MV are known to exhibit unique VQ behavior and show evidence of resultant hypoxia and/or hypercapnia. A small but representative sample of possible VQ distributions has been considered in this paper. In clinical practice, techniques such as MIGET and computerized tomography (CT) can give detailed information regarding the ventilation and perfusion profile of the patient, but these can be expensive to utilize and may not always be readily available, which makes them difficult to use for measurements and monitoring in the ITU. However, VQ distributions are ideally suited to *in silico* investigation and enable us to generate disease scenarios that are representative of a generic case of pathology found in patients requiring MV where the aim is to support patient breathing. The results presented here clearly reveal the huge potential of implementing an optimization-based methodology alongside models of pulmonary physiology that

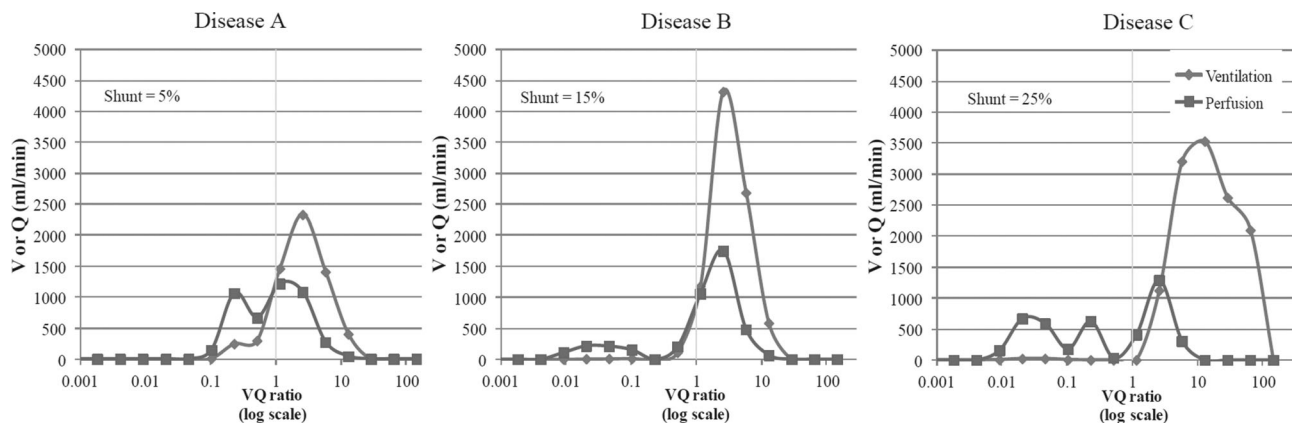


Fig. 8. Ventilation perfusion distribution under optimal settings for each disease state. The effect of optimal MV is evident in the shift of ventilation toward higher VQ ratio.

have previously been used to computationally investigate several clinical problems [31], [32], [46] and have brought real-world advances in clinical care [38], [48].

VII. CONCLUSION

The investigation of systematic approaches for choosing ventilator settings in order to maintain desired blood–gas partial pressures while minimizing the risk factors associated with VALI has been the subject of intense interest in the medical community in recent years. However, there are many factors hampering traditional approaches to research in this area, including 1) the difficulty or impossibility of measuring key patient variables reflecting the effects of MV *in vivo*, 2) the inhomogeneity of physiological responses over time and over the patient population, 3) the number of different ventilator parameters which may be adjusted by the clinician, 4) the lack of clarity over which physiological parameters represent the most important risk factors for VALI, and 5) the ethical constraints on research on patients who are unable to give their own consent. VALI itself has been difficult to diagnose, with limited real time data available, and thus it represents a serious risk to patient welfare. MV input settings also tend to be highly correlated, which can make their effect on internal patient dynamics unpredictable. As a result, limited progress has been made, with ventilator parameters still typically being set using heuristic approaches that are heavily influenced by the clinician’s ability and experience, and large local, national, and international variations existing in treatment protocols.

The results of this study highlight the significant differences which can exist between settings that optimally satisfy the conflicting objectives of MV, even for relatively minor differences in lung compositions (see the optimal settings for disease case A relative to those for the healthy lung). The use of global optimization algorithms to target MV therapy to particular patients, particular diseases, and to particular severity of diseases, would represent significant progress toward the goal of personalized ventilator management for critically ill patients in the modern ITU, where it could help to avoid lung injury, exacerbation of underlying disorders and allow faster recovery from illness.

REFERENCES

- [1] N. Macintyre, “Evolution of the modern mechanical ventilator,” in *Ventilator Management Strategies for Critical Care*, N. S. Hill and M. M. Levy, Eds. New York, NY, USA: Informa Healthcare, 2001, p. 46.
- [2] G. D. Rubenfeld, E. Caldwell, E. Peabody, J. Weaver, D. P. Martin, M. Neff, E. J. Stern, and L. D. Hudson, “Incidence and outcomes of acute lung injury,” *New Engl. J. Med.*, vol. 353, pp. 1685–1693, 2005.
- [3] A. Esteban, A. Anzueto, F. Frutos, I. Alía, L. Brochard, T. E. Stewart, S. Benito, S. K. Epstein, C. Apezteguia, P. Nightingale, A. C. Arroliga, and M. J. Tobin, “Characteristics and outcomes in adult patients receiving mechanical ventilation: A 28-day international study,” *J. Amer. Med. Assoc.*, vol. 287, pp. 345–355, 2002.
- [4] A. Esteban, N. D. Ferguson, M. O. Meade, F. Frutos-Vivar, C. Apezteguia, L. Brochard, K. Raymonds, J. Hurtado, V. Tomacic, J. Elizalde, P. Nightingale, F. Abroug, P. Pelosi, Y. Arabi, R. Moreno, M. Jibaja, G. D’Empaire, F. Sandi, D. Matamis, A. M. Montanez, and A. Anzueto, “Evolution of mechanical ventilation in response to clinical research,” *Am. J. Resp. Crit. Care*, vol. 177, pp. 170–177, 2008.
- [5] M. D. Zilberberg, M. de Wit, J. R. Pirone, and A. F. Shorr, “Growth in adult prolonged acute mechanical ventilation: Implications for healthcare delivery,” *Crit. Care Med.*, vol. 36, pp. 1451–1455, 2008.
- [6] R. Gammon, “Pulmonary barotrauma in mechanical ventilation. Patterns and risk factors,” *Chest*, vol. 102, pp. 568–572, 1992.
- [7] D. Dreyfuss and G. Saumon, “Barotrauma is volutrauma, but which volume is the one responsible?,” *Intensive Care Med.*, vol. 18, no. 3, pp. 139–141, 1992.
- [8] M. Boussarsar, G. Thierry, S. Jaber, F. Roudot-Thoraval, and F. Lemaire, “Relationship between ventilatory settings and barotrauma in the acute respiratory distress syndrome,” *Intensive Care Med.*, vol. 28, no. 4, pp. 406–413, 2002.
- [9] A. Anzueto, F. Frutos-Vivar, A. Esteban, I. Alía, L. Brochard, T. Stewart, S. Benito, M. J. Tobin, J. Elizalde, F. Palizas, C. M. David, J. Pimentel, M. Gonzalez, L. Soto, G. D’Empaire, and P. Pelosi, “Incidence, risk factors and outcome of barotrauma in mechanically ventilated patients,” *Intensive Care Med.*, vol. 30, no. 4, pp. 612–619, 2004.
- [10] V. N. Okamoto and G. D. Rubenfeld, “Attending to the lightness of numbers: Toward the understanding of critical care epidemiology,” *Crit. Care*, vol. 8, pp. 422–424, 2004.
- [11] M. Moss, D. A. Wellman, and G. A. Cotsonis, “An appraisal of multivariable logistic models in the pulmonary and critical care literature,” *Chest*, vol. 123, pp. 923–928, 2003.
- [12] J. Concato, A. R. Feinstein, and T. R. Holford, “The risk of determining risk with multivariable models,” *Ann. Intern. Med.*, vol. 118, pp. 201–210, 1993.
- [13] S. E. Rees, C. Allerod, D. Murley, Y. Zhao, B. W. Smith, S. Kjaergaard, P. Thorgaard, and S. Andreassen, “Using physiological models and decision theory for selecting appropriate ventilator settings,” *J. Clin. Monit. Comp.*, vol. 20, pp. 421–429, 2006.
- [14] G. W. Rutledge, G. E. Thomsen, B. R. Farr, M. A. Tovar, J. X. Polaschek, I. A. Beinlich, L. B. Sheiner, and L. M. Fagan, “The design and implementation of a ventilator management advisor,” *Artif. Intell. Med.*, vol. 5, pp. 67–82, 1993.

- [15] M. Dojat, L. Brochard, F. Lemaire, and A. Harf, "A knowledge-based system for assisted ventilation of patients in intensive care units," *Int. J. Clin. Monit. Comp.*, vol. 9, pp. 239–250, 1992.
- [16] L. Bouadma, F. Lellouche, B. Cabello, S. Taillé, J. Mancebo, M. Dojat, and L. Brochard, "Computer-driven management of prolonged mechanical ventilation and weaning: A pilot study," *Intensive Care Med.*, vol. 31, no. 10, pp. 1446–1450, 2005.
- [17] F. T. Tehrani, "Automatic control of mechanical ventilation. Part 2: The existing techniques and future trends," *J. Clin. Monit. Comp.*, vol. 22, pp. 417–424, 2008.
- [18] F. Tehrani and J. H. Roum, "Flex: A new computerized system for mechanical ventilation," *J. Clin. Monit. Comp.*, vol. 22, no. 2, pp. 121–130, 2008.
- [19] A. K. Gupta, J. Sharma, and P. Mukhopadhyay, "Optimization method applied to the design of ventilators," *Med. Bio. Eng. Comp.*, vol. 16, pp. 387–396, 1978.
- [20] R. Rudowski, A. Bokliden, A. Carstensen, H. Gill, U. Ludwigs, and G. Matell, "Multivariable optimization of mechanical ventilation," *Int. J. Clin. Monit. Com.*, vol. 8, no. 2, pp. 107–115, 1991.
- [21] H. F. Kwok, D. A. Linkens, M. Mahfouf, and G. H. Mills, "SIVA: A hybrid knowledge-and-model-based advisory system for intensive care ventilators," *IEEE Trans. Inf. Technol. Biomed.*, vol. 8, no. 2, pp. 161–172, Jun. 2004.
- [22] A. Wang, M. Mahfouf, G. H. Mills, G. Panoutsos, D. A. Linkens, K. Goode, H. F. Kwok, and M. Denai, "Intelligent model-based advisory system for the management of ventilated intensive care patients, Part II: Advisory system design and evaluation," *Comput. Methods Prog. Bio.*, vol. 99, pp. 208–217, 2010.
- [23] A. Sundaresan, J. G. Chase, G. M. Shaw, Y. S. Chiew, and T. Desai, "Model based optimal PEEP in mechanically ventilated ARDS patients in the intensive care unit," *Biomed. Eng. Online.*, vol. 10, no. 1, pp. 1–18, 2011.
- [24] J. B. West, "Ventilation-perfusion inequality and overall gas exchange in computer models of the lung," *Resp. Physiol.*, vol. 7, no. 1, pp. 88–110, 1969.
- [25] M. Mitchell, *An Introduction to Genetic Algorithms*. Cambridge, MA, USA: MIT press, 1998.
- [26] C. Audet and J. Dennis Jr., "Mesh adaptive direct search algorithms for constrained optimization," *SIAM J. Optimiz.*, vol. 17, no. 1, pp. 188–217, 2007.
- [27] J. G. Hardman, N. M. Bedford, A. B. Ahmed, R. P. Mahajan, and A. R. Aitkenhead, "A physiology simulator: Validation of its respiratory components and its ability to predict the patient's response to changes in mechanical ventilation," *Brit. J. Anaesth.*, vol. 81, pp. 327–332, 1998.
- [28] R. A. McCahon, M. O. Columb, R. P. Mahajan, and J. G. Hardman, "Validation and application of a high-fidelity, computational model of acute respiratory distress syndrome to the examination of the indices of oxygenation at constant lung-state," *Brit. J. Anaesth.*, vol. 101, pp. 358–365, 2008.
- [29] A. Das, Z. Gao, P. P. Menon, J. G. Hardman, and D. G. Bates, "A systems engineering approach to validation of a pulmonary physiology simulator for clinical applications," *J. R. Soc. Interface*, vol. 8, no. 54, pp. 44–55, 2011.
- [30] J. G. Hardman and A. R. Aitkenhead, "Validation of an original mathematical model of CO₂ elimination and dead space ventilation," *Anesth. Analg.*, vol. 97, no. 6, pp. 1840–1845, 2003.
- [31] J. G. Hardman and A. Aitkenhead, "Estimation of alveolar deadspace fraction using arterial and end-tidal CO₂: A factor analysis using a physiological simulation," *Anaesth. Intensive Care.*, vol. 27, pp. 452–458, 1999.
- [32] J. G. Hardman and N. Bedford, "Estimating venous admixture using a physiological simulator," *Brit. J. Anaesth.*, vol. 82, pp. 346–349, 1999.
- [33] P. D. Wagner, R. B. Laravuso, R. R. Uhl, and J. B. West, "Continuous distributions of ventilation-perfusion ratios in normal subjects breathing air and 100% O₂," *J. Clin. Invest.*, vol. 54, pp. 54–68, 1974.
- [34] P. D. Wagner, D. R. Dantzker, R. Duek, J. L. Clusen, and J. B. West, "Ventilation-perfusion inequality in chronic obstructive pulmonary disease," *J. Clin. Invest.*, vol. 59, no. 2, pp. 203–216, 1977.
- [35] P. D. Wagner, D. R. Dantzker, V. E. Iacovoni, W. C. Tomlin, and J. B. West, "Ventilation-perfusion inequality in asymptomatic asthma," *Am. Rev. Respir. Dis.*, vol. 118, no. 3, pp. 511–524, 1978.
- [36] C. G. Elliott, "Pulmonary physiology during pulmonary embolism," *Chest*, vol. 101, pp. 163S–171S, 1992.
- [37] D. Pappert, R. Rossaint, K. Slama, T. Gruning, and J. K. Falke, "Influence of positioning on ventilation perfusion relationships in severe adult respiratory distress syndrome," *Chest*, vol. 106, no. 5, pp. 1511–1516, 1994.
- [38] A. Kathirgamanathan, R. A. McCahon, and J. G. Hardman, "Indices of pulmonary oxygenation in pathological lung states: An investigation using high-fidelity, computational modelling," *Brit. J. Anaesth.*, vol. 103, no. 2, pp. 291–297, 2009.
- [39] A. B. Dubois, S. Y. Botelho, and J. H. Comroe, "A new method for measuring airway resistance in man using a body plethysmograph: Values in normal subjects and in patients with respiratory disease," *J. Clin. Invest.*, vol. 35, no. 3, pp. 327–335, 1956.
- [40] R. Naeije, "Should pulmonary hypertension be treated in chronic obstructive pulmonary disease," in *Diagnosis and Treatment of Pulmonary Hypertension*, E. K. Weir, S. L. Archer, and J. T. Reeves, Eds. Mt. Kisco, NY, USA: Futura, 1992, pp. 209–239.
- [41] T. De Campos, "Ventilation with lower tidal volumes as compared with traditional tidal volumes for acute lung injury and the acute respiratory distress syndrome: The acute respiratory distress syndrome network," *New Engl. J. Med.*, vol. 342, no. 18, pp. 1301–1308, 2000.
- [42] J. Villar, L. Perez-Mendez, J. Lopez, J. Belda, J. Blanco, I. Saralegui, S. Suarez-Sipman, S. Lubillo, and R. M. Kacmarek, "An early PEEP/FIO₂ trial identifies different degrees of lung injury in patients with acute respiratory distress syndrome," *Am. J. Resp. Crit. Care*, vol. 176, no. 8, pp. 795–804, 2007.
- [43] A. Esteban, A. Anzueto, I. Alia, F. Gordo, C. Apezteguia, F. Palizas, D. Cide, R. Goldwaser, L. Soto, G. Bugedo, C. Rodrigo, J. Pimentel, G. Raimondi, and M. J. Tobin, "How is mechanical ventilation employed in the intensive care unit," *Am. J. Respir. Crit. Care Med.*, vol. 161, pp. 1450–1458, 2000.
- [44] K. Deb, A. Pratap, S. Agarwal, and T. Meyarivan, "A fast and elitist multiobjective genetic algorithm: NSGA-II," *IEEE Trans. Evol. Comput.*, vol. 6, no. 2, pp. 182–197, Apr. 2002.
- [45] F. Feihl and C. Perret, "Permissive hypercapnia. How permissive should we be?," *Am. J. Resp. Crit. Care*, vol. 150, no. 6, pp. 1722–1737, 1992.
- [46] J. S. Wills and J. G. Hardman, "The development of hypoxaemia during apnoea in children: A computational modelling investigation," *Brit. J. Anaesth.*, vol. 97, no. 4, pp. 564–570, 2006.
- [47] S. McClelland, D. Bogod, and J. G. Hardman, "Pre-oxygenation and apnoea in pregnancy: Changes during labour and with obstetric morbidity in a computational simulation," *Anaesthesia*, vol. 64, no. 4, pp. 371–377, 2009.
- [48] H. Al-oataibi and J. G. Hardman, "Prediction of arterial oxygen tension: Validation of a novel formula," *Am. J. Resp. Crit. Care*, vol. 182, no. 3, pp. 435–436, 2010.

Authors' photographs and biographies not available at the time of publication.